Virology 468-470 (2014) 621–630

Contents lists available at ScienceDirect

Virology

journal homepage: www.elsevier.com/locate/yviro

Recombinant rabies virus expressing IFNα1 enhanced immune responses resulting in its attenuation and stronger immunogenicity

Yifei Wang [a,1], Qin Tian [a,1], Xiaojuan Xu [a,2], Xianfeng Yang [a,3], Jun Luo [a], Weiyu Mo [a], Jiaojiao Peng [a], Xuefeng Niu [b], Yongwen Luo [a], Xiaofeng Guo [a,*]

[a] College of Veterinary Medicine, South China Agricultural University, Guangzhou, China
[b] The First Affiliated Hospital, Guangzhou Medical University, Guangzhou, China

ARTICLE INFO

Article history:
Received 31 July 2014
Accepted 9 September 2014
Available online 11 October 2014

Keywords:
Rabies virus
Interferon
Vaccine

ABSTRACT

Several studies have shown that type 1 interferons (IFNs) exert multiple biological effects on both innate and adaptive immune responses. Here, we investigated the pathogenicity and immunogenicity of recombinant rabies virus (RABV) expressing canine interferon α1 (rHEP-CaIFNα1). It was shown that Kun Ming (KM) mice that received a single intramuscular immunization with rHEP-CaIFNα1 had an earlier increase and a higher level of virus-neutralizing antibody titers compared with immunization of the parent HEP-Flury. A challenge experiment further confirmed that more mice that were immunized with rHEP-CaIFNα1 survived compared with mice immunized with the parent virus. Quantitative real-time PCR indicated that rHEP-CaIFNα1 induced a stronger innate immune response, especially the type 1 IFN response. Flow cytometry was conducted to show that rHEP-CaIFNα1 recruited more activated B cells in lymph nodes and CD8 T cells in the peripheral blood, which is beneficial to achieve virus clearance in the early infective stage.

Introduction

Rabies is an ancient zoonosis that still accounts for 55,000 human deaths annually, most of which occur in developing regions of the world (World Health Organization, 2010). Rabies virus enters neurons at peripheral sites and travels through the spinal cord to the brain of the infected host, often inducing aggression that facilitates the transfer of virus to a new host (Schnell et al., 2009). Rabies has a high associated mortality rate, and thus, an effective vaccine plays a vital role in controlling rabies outbreaks. Animal vaccination barriers should be set up to prevent human rabies because human infections occur through contact with rabid domestic dogs or other canidae (Hicks et al., 2012). Rabies virus (RABV) itself is a favorable vaccine vector. Much research has been focused on the application of recombinant RABV (rRABV) expressing foreign proteins (Gomme et al., 2011; Verardi et al., 2012; Yilma et al., 2010). Expression of multiple copies of RABV G (Schutsky et al., 2013; Liu et al., 2014; Zhang et al., 2012) and expression of some immune-related genes (Wang et al., 2011; Wen et al., 2011; Zhao et al., 2010) have also been confirmed to lead to enhanced immunogenicity and viral attenuation. As a vital innate-response gene, interferon (IFN), especially type 1 interferon (IFN1), not only enhances antigen presentation and the production of immune response mediators, such as cytokines and chemokines, but also affects adaptive immunity. For example, type 1 IFNs can augment antibody production by B cells and amplify the effector function of T cells (Ahlenstiel et al., 2011; Ivashkiv and Donlin, 2014; Kohlmeier et al., 2010; Staudt et al., 2010).

According to our previous study, appropriate doses of canine interferon α1 enhanced the immunogenicity of rabies vaccine when they were administered simultaneously in dogs (data not shown). Type 1 interferon possessed the characteristic of species specificity, and canine interferon α subtypes showed much lower antiviral activity on the bovine, swine, rabbit, and feline cells than canine cell (Taira et al., 2005). The activity of CaIFNα1 in mouse was investigated via detecting the activation of STAT1 in murine cells by immunofluorescence microscopy. We found that the higher level of pSTAT1(Y701) was detected in BSR, NA, and Balb/c-3T3 cells after treatment with CaIFNα1, which indicates that mouse is sensitive to CaIFNα1 and makes it permissible to use mouse model in our earlier animal experiment. In this study, the

* Corresponding author.
E-mail address: xfguo@scau.edu.cn (X. Guo).
[1] Yifei Wang and Qin Tian contributed equally to this work.
[2] Present address: Bureau of Animal Husbandry and Food Administration of Cangxi, Sichuan, China.
[3] Present address: Key Laboratory of Rubber Biology of the Ministry of Agriculture, Rubber Research Institute, Chinese Academy of Tropical Agricultural Sciences, Danzhou, Hainan, China

http://dx.doi.org/10.1016/j.virol.2014.09.010
0042-6822/

recombinant high egg passage Flury strain (HEP-Flury) of RABV that contains the canine interferon α1 gene (rHEP-CaIFNα1) was investigated in mouse. Our study indicated that recombinant RABV not only decreases the pathogenicity but also increases the immunogenicity of RABV.

Results

Recombinant RABV construction

Insertion of the canine IFNα1 gene was confirmed by sequencing the fragment with the infectious clones. Recombinant RABVs were rescued using the procedures described by Inoue et al. (2003) and designated rHEP-CaIFNα1 (Fig. 1A)

rRABV in vitro characterization

To characterize the rRABV in vitro, viral growth kinetics were examined in BSR cells and NA cells. As shown in Fig. 1B, difference between the values was observed between recombinant virus and the parental virus, indicating that there is effect on viral growth caused by the insertion of the CaIFNα1 gene. The restriction effect of canine interferon on viral replication seemed much stronger in NA cells than BSR cells, which indicated that NA cells were more sensitive to interferon. The ability of the rHEP-CaIFNα1 to produce CaIFNα1 was determined by measuring CaIFNα1 in virus-infected BSR cells using an ELISA kit. As shown in Fig. 1C, CaIFNα1 was produced by rHEP-CaIFNα1 in a dose-dependent manner. No CaIFNα1 product was detected in the supernatant of BSR cells infected with the parent virus HEP-Flury.

Immunofluorescence microscopy

Interferon initials the host antiviral response via JAK/STAT signaling pathway. The phosphorylation of STAT1 indicated activity of interferon in host cells. As shown in Fig. 2, pSTAT1(Y701) was highly expressed in three kinds of mouse cells incubated with CaIFNα1 than mock control, which was suggested that mouse is sensitive to CaIFNα1.

Apoptosis detection

It has been shown that expression of IFN induces apoptosis (Kalliolias and Ivashkiv, 2010; Kotredes and Gamero, 2013). An Annexin V-FITC Apoptosis Detection Kit (Keygentec, China) was used to detect apoptosis in our study. As shown in Fig. 3, the early apoptotic cells (Annexin V-FITC-positive and PI-negative) were located in the lower right quadrant. The late apoptotic or necrotic cells (Annexin V-FITC-positive and PI-positive) were located in the upper right quadrant. The healthy cells (negative for both probes) were located in the lower left quadrant. The results are represented as the percentage of Annexin V-FITC-positively- and PI-negatively-stained cells (located in lower right quadrant) among total cells. As our data showed, the induction of apoptosis in cultured cells (both NA cells and BSR cells) infected with rHEP-CaIFNα1 was significantly higher than cultured cells infected with parent virus.

rRABV's pathogenicity in mice

According to the method described above, infected mice were monitored daily for 4 weeks for weight changes, for development of disease, and for death. When infected with HEP-Flury at the doses of 10^5 FFU, infected mice lost more body weight than when they were infected with rHEP-CaIFNα1 (Fig. 4). Most of the mice regained their prechallenge body weight by 16 days post-infection (dpi) when they were infected with rHEP-CaIFNα1, while the mice infected with HEP-Flury did not regain their prechallenge body weight until 25 dpi (Fig. 4). No overt clinical symptoms, such as abnormal behaviors, or any neurological signs, were observed among these mice. These data indicated that recombinant RABVs carrying CaIFNα1 did not increase RABV virulence, but that they reduced viral pathogenicity.

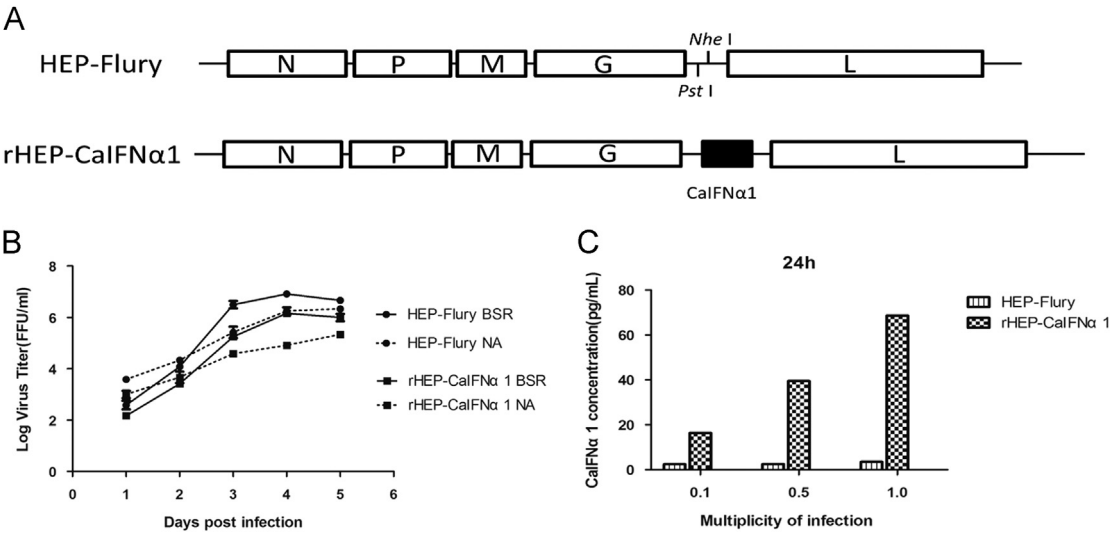

Fig. 1. Construction of recombinant RABV and characterization of rRABV in vitro. (A) Recombinant RABV is constructed as described in *Materials and methods*. N, nucleoprotein; P, phosphoprotein; M, matrix protein; G, glycoprotein; L, RNA-dependent RNA polymerase. (B) Virus growth curves in BSR and NA cells. Virus growth curves are determined by infecting BSR cells (solid line) or NA cells (dashed line) with either the HEP-Flury or rHEP-CaIFNα1 virus at a multiplicity of infection (MOI) of 0.01. At days 1, 2, 3, 4, and 5 after infection, the culture supernatants are harvested, and viral titers are determined. (C) CaIFNα1 expression in cells culture supernatants. CaIFNα1 expression is determined using infected BSR cells with either the rHEP-CaIFNα1, or HEP-Flury at an MOI of 0.01, 0.1, or 1. After incubation at 34 °C for 24 h, the culture supernatants are harvested, and the amounts of CaIFNα1 are determined using a canine IFNα enzyme-linked immunosorbent assay (ELISA) kit, according to the manufacturer's instructions. The positive control (CaIFNα) is supplied with the kit.

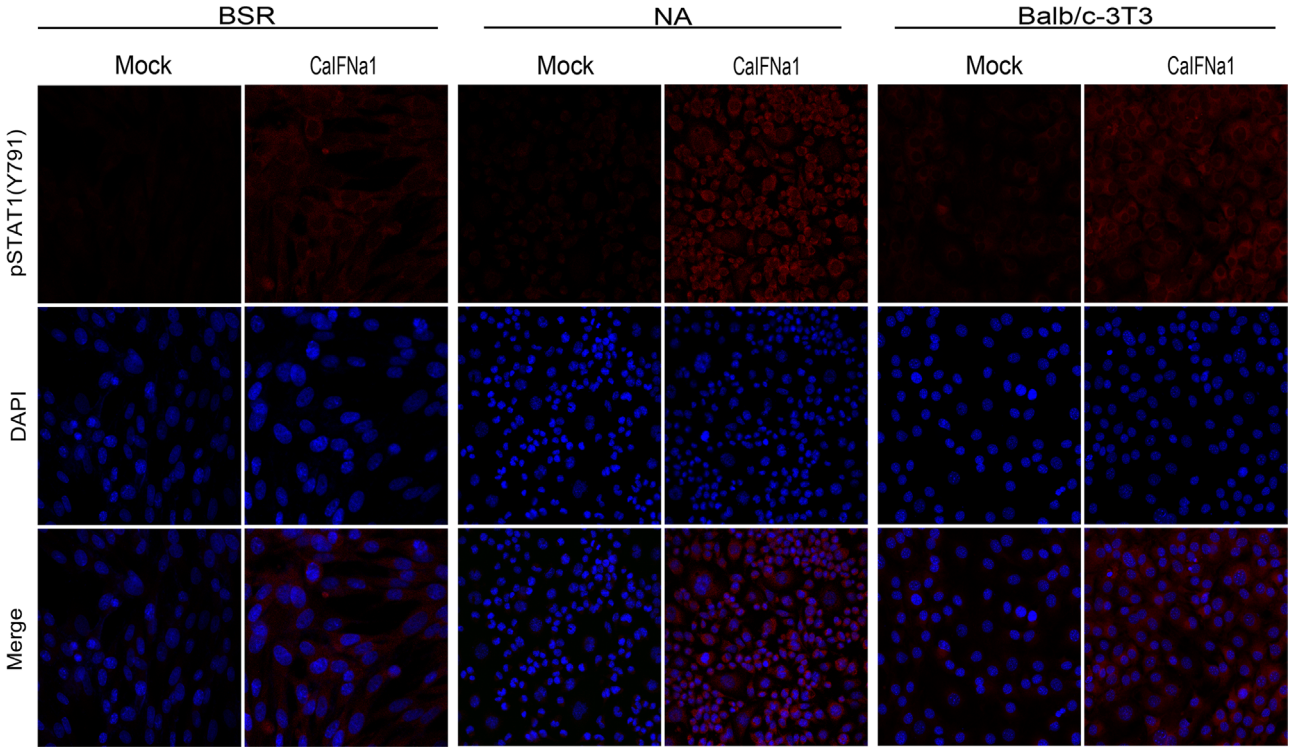

Fig. 2. Immunofluorescence microscopy. BSR cells, NA cells, Balb/c-3T3 cells are cultured in a glass bottom cell culture dish and incubated with 100 U/ml CalFNα1 at 37 °C for 1 h. Mock treatment is conducted by inoculation with DMEM. After incubation, the cells are fixed and permeabilized in 0.5% TritonX-100 in phosphate-buffered saline (PBS). The cells are then stained with pSTAT1(Y701)-PE and DAPI. Confocal laser scanning microscopy is performed with a Zeiss LSM780 laser system using a Zeiss LSCM 7DUO microscope. Excitation of Alexa Flour 488 nm, PE and DAPI occurred at wavelengths of 575 nm, and 460 nm, respectively.

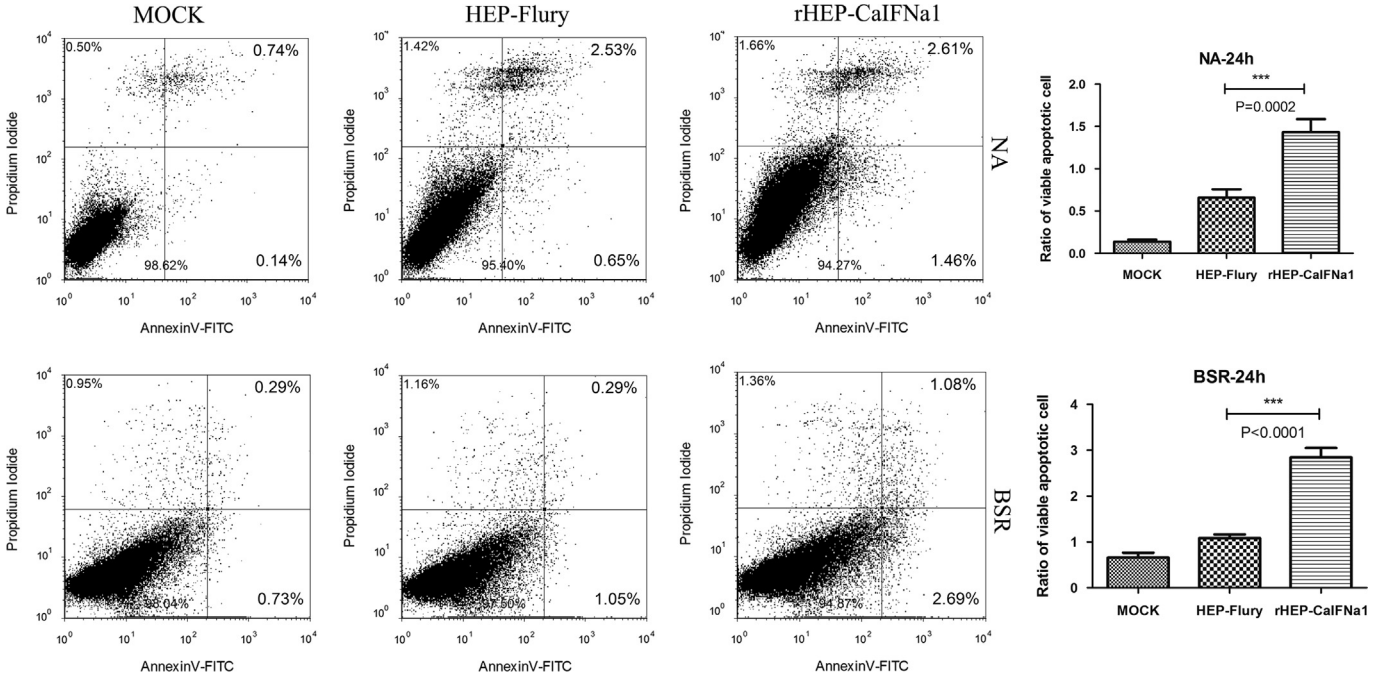

Fig. 3. Apoptosis detection. Annexin V-FITC and PI staining for flow cytometry detection of apoptosis of NA and BSR cells induced by HEP-Flury and rHEP-CalFNα1. The cells are incubated with virus for 24 h prior to being stained with Annexin V-FITC and PI. The early apoptotic cells (Annexin V-FITC+ and PI−) are located in the lower right quadrant. The results are represented as the percentage of Annexin V-FITC+ and PI− cells among total cells.

rRABV's immunogenicity

Each group of mice ($n=10$) was immunized once via the intramuscular route with different doses of rHEP-CalFNα1 or HEP-Flury (5×10^2, 5×10^3, or 5×10^4 FFU per mouse). Blood samples were collected at 7 dpi, 14 dpi, and 21 dpi, and serum was used for determination of VNA using ELISA. Overall, the level of VNA is dose dependent for all viruses. Fig. 5A, B, and C show the VNA levels in immunized mice at 7 dpi, 14 dpi, and 21 dpi, respectively. A level of 0.5 international units (I.U.) is considered

protective from RABV infection. The level of VNA was under 0.5 IU in mice immunized with all the viruses at 7 dpi although significantly higher level of VNA was detected in mice immunized with rHEP-CaIFNα1 than with HEP-Flury. Significantly higher VNA titers were also detected in mice immunized with rHEP-CaIFNα1 than in those induced by immunization with the parent virus, and HEP-Flury, at both 14 dpi and 21 dpi, respectively. To investigate if the higher VNA titers correlate with better protection, immunized mice were then challenged with 50 LD50 of virulent CVS-24 via intracranial route on day 23 after vaccination and observed for development of disease and death for 2 weeks. As shown in Fig. 6, significantly more survivors were observed among those immunized with rHEP-CaIFNα1 than among those immunized with the parent HEP-Flury virus, when the smaller doses (5×10^2 and 5×10^3 FFU per mouse) were used. More survivors were also observed among mice immunized with rHEP-CaIFNα1 than among mice immunized with the HEP-Flury, but no significant difference was detected with the dose of 5×10^4 FFU per mouse. Taken together, these data indicate that rRABV expressing CaIFNα1 provides better protective immunity than the parent virus.

Induction of innate immune responses and viral growth in vivo

To investigate the ability of the rHEP-CaIFNα1 to induce innate immune responses, especially the type 1 IFN response, BALB/c mice were infected with 10^5 FFU of each virus by intramuscular route, and at 3 dpi or 6 dpi, mice were humanely sacrificed and muscle harvested for measuring the expression of interferon-induced genes (IIGP1, IRF3, ISG20, MusIFNα1, PDCD4, and STAT1) using quantitative real-time PCR as described above. Details are shown in Fig. 7. We found that rHEP-CaIFNα1 induced much stronger interferon-related innate immune response in immunized mice than HEP-Flury. On the other hand, there was no difference in the fold changes of PDCD4 (Programmed Cell Death 4) compared with that of control RABV, which indicated that rHEP-CaIFNα1 did not cause more apoptosis than the parent HEP-Flury virus. No activation of apoptosis during in vivo study might be due to the low level of virus replication and IFN production at the site of inoculation, as shown in Fig. 7. Data showed that the rHEP-CaIFNα1 N mRNA expression level was much lower than parent HEP-Flury virus, which indicated that the interferon responses induced by rHEP-CaIFNα1 obstructed the viral replication in vivo.

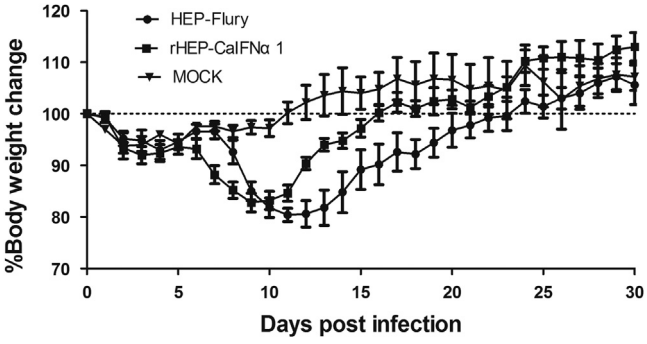

Fig. 4. Body weight change of mice infected with recombinant RABV. The pathogenicity of recombinant rHEP-CaIFNα1 is determined by infecting BALB/c mice (6–7 weeks of age) intracranially with 10^5 FFU of either the HEP-Flury, rHEP-CaIFNα1 virus or with medium alone (mock infection). Body weight is monitored daily. Data are obtained from 5 mice in each group and presented as the mean value ± standard error (SE).

Effects of rRABV on the recruitment of B and T cells

To determine if the expression of interferon-induced genes results in influence on the recruitment of B and T cells, flow cytometry was performed to quantify the immune cells in the peripheral blood and lymph nodes. The populations of activated B cells in the inguinal lymph node were differentiated using the cell surface markers CD19 and CD40. The populations of CD4 T cells and CD3 T cell in the peripheral blood were differentiated using CD4 and CD8, respectively, while CD3 was used as a maker for all T cells. Fig. 8A shows representative flow cytometric plots of CD4 T cells (CD3-positive and CD4-positive) and CD8 T cells (CD3-positive and CD8-positive), and Fig. 8C shows plots of B cells (CD19-positive and/or CD40-positive) at days 3, 5, or 7 after infection with each RABV. As shown in Fig. 8B and D, more immune cells (CD8 T cells as detected by CD8 and CD3 and activated B cells as detected by CD19 and CD40) were detected in mice infected with rHEP-CaIFNα1 than in mice infected with the parent virus.

Discussion

Recent studies showed that the activation of innate immune responses is one of the mechanisms by which RABV is attenuated (Leroy et al., 2006). Chemokine overexpression can be a benefit if the expression is transient, but it can be harmful to the host if the expression is persistent during RABV infections (Kuang et al., 2009; Niu et al., 2011). Interferon, synthesized and secreted from infected cells, in turn directed amplification of the response and transcription of a broader range of antiviral genes in both autocrine and paracrine manners, leading to establishment of an antiviral state. Type 1 IFN responses are fine-tuned by host factors (Ivashkiv and Donlin, 2014), which make them promising biologicals to enhance the immune effect. Similar to other viruses, RABV has evolved effective mechanisms to obstruct the anti-viral

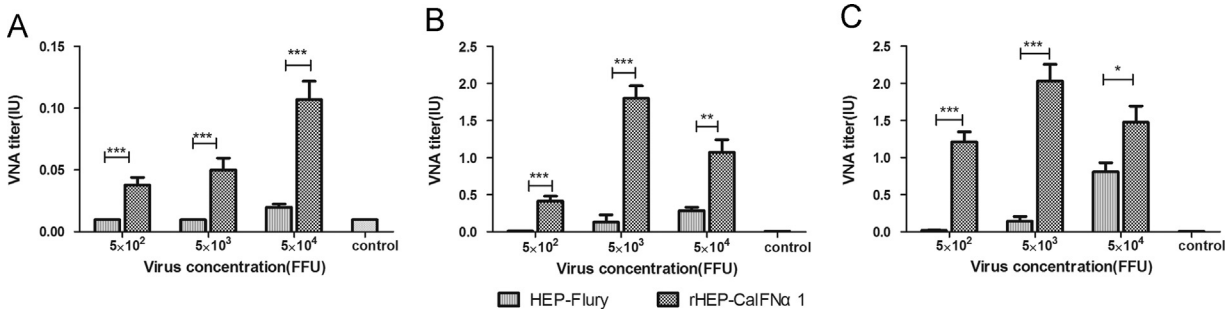

Fig. 5. VNA titers in mice immunized with recombinant RABV. Groups of 10 KM mice (6–7 weeks of age) are immunized via the intramuscular route with serial 10-fold dilutions of HEP-Flury, or rHEP-CaIFNα1. At days 7 (A), 14 (B), and 21 (C) after immunization, the peripheral blood is obtained, and the serum is used to determine VNA titers, using the ELISA assay, according to the manufacturer's instructions. A level of 0.5 international units (I.U.) is considered protective from RABV infection. Data are analyzed using GraphPad Prism 5. Asterisks indicate significant differences among the experimental groups, as calculated by one-way ANOVA (*$p<0.05$; **$p<0.01$; ***$p<0.001$).

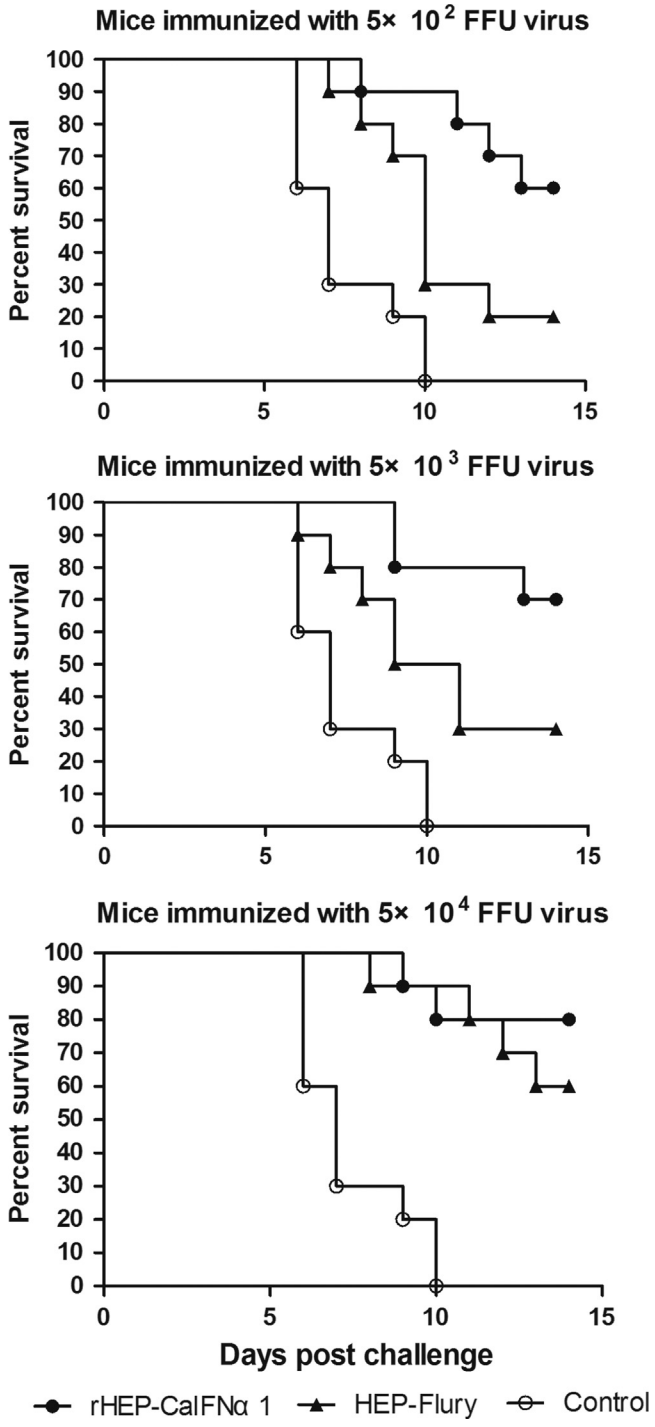

Fig. 6. Survivorship curves of mice challenged with CVS24. Mice immunized with either HEP-Flury, rHEP-CaIFN, or DMEM (control) are challenged via the intracranial route with 50 LD_{50} of CVS24 on day 23 after immunization and observed daily for 2 weeks. The number of survivors is recorded and compared. Data are analyzed using GraphPad Prism 5 with Gehan–Breslow–Wilcoxon Test or Log-rank (Mantel–Cox) Test. The difference in survival between mice immunized with rHEP-CaIFNα1 and mice immunized with HEP-Flury is significant when the smaller doses (5×10^2 and 5×10^3 FFU per mouse) are used ($p < 0.05$).

responses in the host (Randall and Goodbourn, 2008). In previous studies, RABV phosphoprotein P was confirmed to be an IFN antagonist that plays a major and multifunctional role in disturbing interferon gene expression, interferon-induced STAT signaling, and the functions of antiviral protein (Lieu et al., 2013; Vidy et al., 2007; Wiltzer et al., 2014). Although RABVs have developed advanced countermeasures against the IFN system, the interferon-mediated mechanisms are still the main factors restricting RABV replication in vivo (Carty et al., 2014; Faul et al., 2009; Lafon, 2011; Schoggins et al., 2011). Lafon et al. showed that although the neuroinvasive RABV strain CVS-NIV reduces type 1 IFN signaling, an early and transient type 1 IFN response is still triggered in the infected neuronal cells and nervous system (NS) (Carty et al., 2014), and this type 1 IFN response is efficient enough to reduce neuroinvasiveness and pathogenicity and partially protect the host from fatal infection (Chopy et al., 2011). Faul et al. constructed a recombinant rabies virus expressing both IFN-β and HIV-1 Gag. The rRABV expressing IFN-β (IFN+) is highly attenuated and the mice immunized with IFN+ RABV had a significantly greater number of activated CD8 T cells, which indicated that interferon expressed by rabies virus-based HIV-1 vaccine vector could serve as a molecular adjuvant (Faul et al., 2008).

In the present study, the recombinant RABV rHEP-CaIFNα1 was investigated and compared with the parent HEP-Flury virus. The viral titers of recombinant RABV were slightly lower than those of the parent virus in BSR cells and much lower than those of the parent virus in NA cells (Fig. 1B). The BSR cells cannot produce IFN (Marschalek et al., 2009; Rieder and Conzelmann, 2011) but have an IFN-α/β receptor. Infection of RABV stimulated the responses of IFN, and viral replication of rHEP-CaIFNα1 could be inhibited for this reason in BSR cells (Niu et al., 2013). In NA cells, which are IFN-competent, the restriction effect of IFN on viral replication was much stronger.

Our study indicated that pSTAT1(Y701) was higher expressed in mouse cells incubated with CaIFNα1 than mock control (Fig. 2). After being confirmed its sensibility to CaIFNα1, mouse was used to investigate the pathogenicity and immunogenicity of rHEP-CaIFNα1. Mice infected with rHEP-CaIFNα1 regained their body weight sooner than the other mice that were infected with HEP-Flury (Fig. 4). Although body weight loss occurred, mice infected with both the parent virus and rHEP-CaIFNα1 did not show overt clinic symptoms, abnormal behavior, or any neurological signs. Besides, it was shown that mice infected with rHEP-CaIFNα1 suffered less body weight loss than mice infected with the parent virus. The result indicated that CaIFNα1 expression reduced the rRABV pathogenicity.

A higher VNA level (Fig. 5) and better protection (Fig. 6) were detected among mice immunized with the recombinant virus than among mice immunized with the parent virus. In addition, the mice immunized with recombinant RABV responded to viral infection sooner than mice immunized with a parent virus. Another characteristic of the rRABV is that a relatively small dose of rHEP-CaIFNα1 is needed to induce sufficient VNA and show effective protection. As our data showed, when the smaller immunized doses (5×10^2 and 5×10^3 FFU per mouse) were used, significantly more survivors were observed among those immunized with rHEP-CaIFNα1 than among those immunized with the parent HEP-Flury virus (Fig. 6).

In order to investigate the mechanism of how rHEP-CaIFNα1 enhances immunogenicity and viral attenuation, interferon-induced gene expression at the inoculation site is evaluated using quantitative real-time PCR. Our data showed that the recombinant RABV rHEP-CaIFNα1 induced a stronger innate immune response in mice with the higher expression level of ISG20, IIGP1, IRF3, and STAT1 (Fig. 8A). ISG-encoded proteins restrain pathogens via several mechanisms including inhibiting viral transcription, translation and replication; degrading viral nucleic acids; and altering cellular lipid metabolism (Degols et al., 2007). IIGP1 belongs to a well-defined family of 47-kDa GTPase whose members are present at low resting levels in mouse cells, but are strongly induced transcriptionally by interferons, and are implicated in cell-autonomous resistance to intracellular pathogens (Uthaiah et al., 2003). IRF3 was

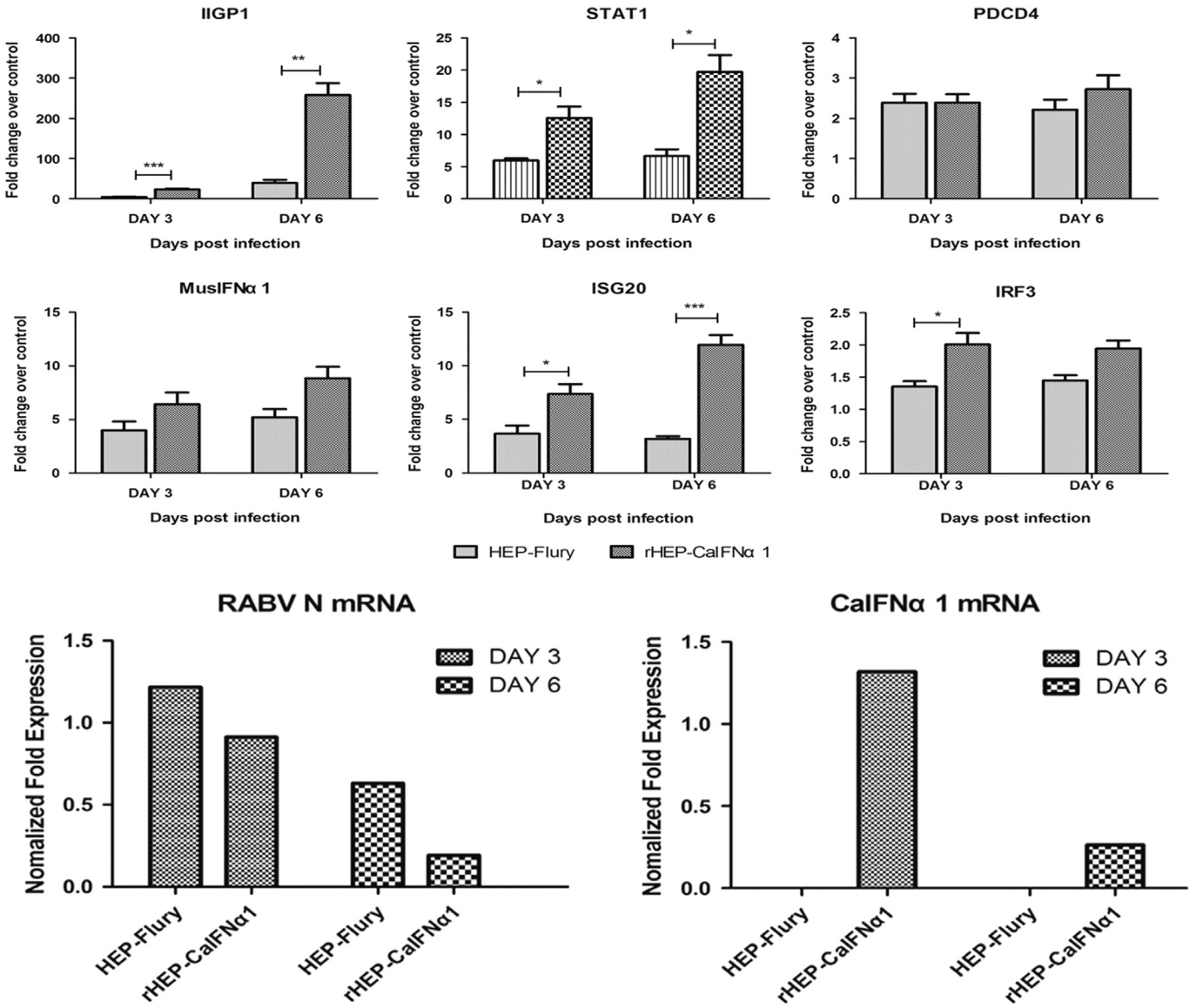

Fig. 7. Expression of interferon-related immune genes. BALB/c mice are infected with 10^5 FFU of each virus via the intramuscular route, and at 3 dpi or 6 dpi, mice are sacrificed humanely and muscles are harvested for measuring the expression of interferon-related genes (STAT1, IRF3, IIGP1, PDCD4, ISG20, and MusIFNα1) by quantitative real-time PCR in a CFX384 Real-Time System. The expression levels of target genes, IIGP1, IRF3, PDCD4, STAT1, and mouse interferon alpha (MusIFNα1), are normalized to those of reference gene glyceraldehyde-3-phosphate dehydrogenase (GAPDH). The RABV N mRNA and CaIFNα1 mRNA are quantitated relative to the GAPDH expression level. Data are analyzed using BioRadCFX Manager and GraphPad Prism 5. Asterisks indicate significant differences among the experimental groups, as calculated by one-way ANOVA ($^*p < 0.05$; $^{**}p < 0.01$; $^{***}p < 0.001$).

found to be essential for MAVS/IPS-1-directed ISG transcription and IFN-β secretion during virus infection (Sen et al., 2011; Zhang et al., 2013). As an important component of the type 1 IFN signaling pathway, STAT1 is widely expressed and thus most cell types are competent to mount type 1 IFN-dependent responses with other necessary components, such as IFNAR, JAK1, TYK2, STAT2, and IRF9. On the other hand, the magnitude of this signaling is balanced by opposing mechanisms that limit expression of IFNAR-JAK-STAT signaling components (Ivashkiv and Donlin, 2014). Though the induction of apoptosis in cultured BSR and NA cells infected with rHEP-CaIFNα1 was significantly higher than that infected with parent virus, the PDCD4 (Programmed Cell Death 4) level induced by rHEP-CaIFNα1 was similar to that of HEP-Flury, which may due to the low level of virus replication and IFN production at the site of inoculation. This indicated that rHEP-CaIFNα1 did not tend to deepen the degree of apoptosis in vivo, which may cause organism damage, compared with the parent HEP-Flury virus (Baloul and Lafon, 2003; Subedi et al., 2013). The interferon responses induced by rHEP-CaIFNα1 also impacted the viral replication in vivo (Chopy et al., 2011). The relative quantity of RABV N mRNA (relative to reference gene GAPDH) among mice infected with rRABV expressing CaIFNα1 was analyzed. As shown in Fig. 7, rHEP-CaIFNα1 N mRNA expression was lower than parent HEP-Flury virus, suggesting that interferon-induced responses interfered the viral growth in mice.

Our study indicated that the recombinant RABV expressing IFNα1 (rHEP-CaIFNα1) recruited and/or activated more B cells or CD8 T cells in lymph nodes or the peripheral blood than did the parent virus, which may be related to interferon-induced innate responses and the reduction of viral load at an early rRABV infection stage (Fig. 8). Because CD19 and CD40 are B cell-specific surface markers that are present in the pre-B cells, the immature B cell and mature B cell surfaces are associated with B cell activation (Castigli et al., 1996), and CD19-PerCP and CD40-FITC were used to detect activated B cells in our study. Our data suggest that activated B cells are recruited in lymph nodes of mice

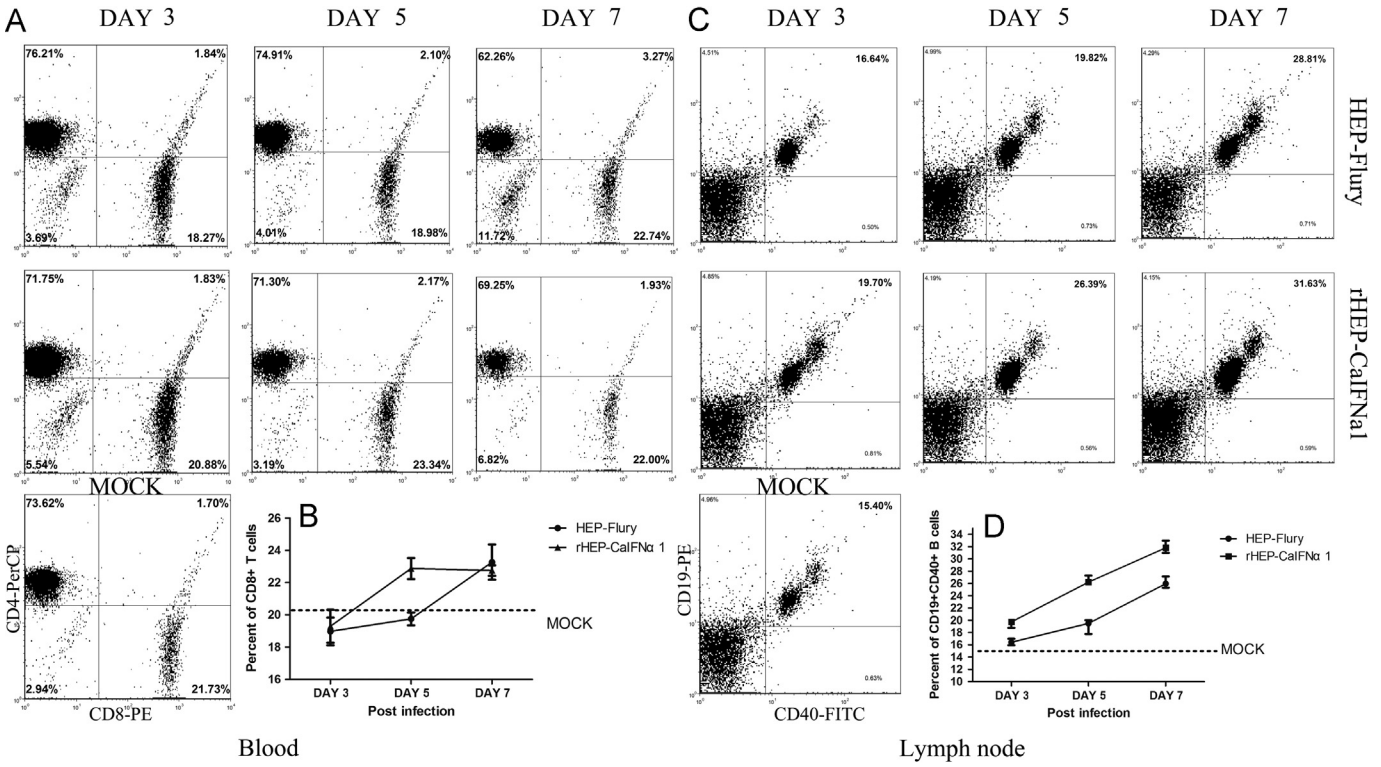

Fig. 8. Recruitment and activation of CD8 T cells and B cells. BALB/c mice are infected via the intramuscular route with 1×10^5 FFU rHEP-CaIFNα1 or HEP-Flury, and peripheral blood or inguinal lymph nodes are harvested at 3, 5, and 7 days post-infection. Single-cell suspensions are prepared and stained with antibodies to T cell markers (CD3-FITC, CD8-PE, and CD4-PerCP) or B cell markers (CD19-PE and CD40-FITC). Data collection and analysis are performed using a Beckmen FC 500 flow cytometer and FCS Expression software. (A) CD3-FITC is used to gate all T cells in the blood. The plots in lower-right quadrant of each scatter plot represent $CD3^+CD8^+$ cells. (B) The line chart shows differences in the magnitude of CD8 T cell recruitment at days 3, 5, and 7 with the rRABV and parent virus. (C) The plots in upper-right quandrant of each scatter plot represent $CD19^+CD40^+$ B cells. (D) The line chart shows the different magnitude of recruitment and/or activation of B cells at days 3, 5, and 7 with the rRABV and parent virus.

immunized with rHEP-CaIFNα1, and induce interferon responses that are greater than parent virus at 3 dpi, 5 dpi and 7 dpi, suggesting that recombinant RABV induced a stronger and quicker response in immunized mice in the early infective stage (Braun et al., 2002; Fink et al., 2006; Le Bon et al., 2006). The percent of $CD3^+CD8^+$ T cells in blood among mice immunized with rHEP-CaIFNα1 maintained higher level than mock at day 7 post-inoculation, while the $CD3^+CD8^+$ T cells in blood among mice immunized with parent HEP-Flury virus just started their upward momentum. This result may be relevant to the reduction of viral load in mice infected with rHEP-CaIFNα1 that induce interferon responses (Fig. 7). As previous studies suggested, the elaboration of the anti-viral CD8 T cell responses following infection is a cornerstone of the adaptive immune responses, and they are vital for controlling acute infections, containing persistent infections, and conferring long-lived protection to viral re-exposures (Carty et al., 2014; Zhang and Bevan, 2011). The increased CD8 T cell response to the infection was considered to be beneficial. In addition, our data showed that rHEP-CaIFNα1 recruited more $CD19^+CD40^+$ B cells in lymph nodes among immunized mice than parent virus, which may contribute to the higher VNA induced by rHEP-CaIFNα1 than the parental virus. The stronger response of immune cells may be related to the enhanced immunogenicity and reduced pathogenicity of recombinant RABV (Cox et al., 2013; Le Bon et al., 2006).

The immunization in dogs is on the schedule, and the outlook of application in emergency treatment after exposure is also promising. In summary, our studies demonstrate that IFNα1 expression results not only in reduced RABV pathogenicity but also in enhanced RABV immunogenicity by affecting the innate and adaptive immunity in mice. Recombinant RABV that expresses CaIFNα1 has the potential to be developed as an avirulent RABV vaccine.

Materials and methods

Cells, virus, antibodies, and animals

BSR cells and BHK-21 cells were maintained in Dulbecco's modified Eagle's medium (DMEM) (Gibco, Invitrogen, China) containing 10% FBS. rRABV was rescued in BHK-21 cells and propagated in BSR cells. Challenge virus standard 24 (CVS-24) was propagated in sucking mice brains. Fluorescein isothiocyanate (FITC)-conjugated antibody against the RABV N protein was purchased from Fujirabio Inc., Malvern, PA. Antibodies used for flow cytometric analysis or immunoflourescen microscopy, such as CD4-PerCP(RM4-5), CD8a-PE(53-6.7), CD3e-FITC (145-2C11), CD19-FITC(1D3), CD40-PE(3/23), and pSTAT1(Y701)-PE(4a), were purchased from BD Pharmingen (USA). Annexin V-FITC Apoptosis Detection Kit (Keygentec, China) was used to detect the early apoptotic cells after infection with rabies virus. Female BALB/c and KM mice were purchased from Center for Laboratory Animal Science, Southern Medical University and housed in the animal facility of the College of Veterinary Medicine, South China Agricultural University. All animal experiments were carried out in compliance with national standard Laboratory Animal Requirements of Environment and Housing Facilities (CALAS, GB 14925-2001) and following Guidelines on the Humane Treatment of Laboratory Animals.

Construction of recombinant RABV cDNA clones

High egg passage Flury strain (HEP-Flury) of RABVs was used as the parent RABV. Based on the HEP-Flury, a recombinant RABV infectious clone was constructed by inserting CaIFNα1 between G and L genes to obtain rHEP-CaIFNα1.

Rescue of recombinant RABV from cloned cDNA

Recombinant RABVs were rescued as described previously (Inoue et al., 2003). Briefly, BHK-21 cells grown in 12-well plates were transfected with 1.25 μg of the full-length clone and 0.3125 μg, 0.15625 μg, 0.09375 μg, and 0.0625 μg of pcDNA-N, -P, -G and -L, respectively using 7.5 μl of SuperFect transfection reagent (Qiagen, GER) in a final volume of 75 μl. The transfection was allowed to proceed for 3 h and then the transfecting medium was removed and replaced with fresh DMEM containing 10% FBS. After incubation at 37 °C for 2 days, the culture medium was removed and fresh medium with 5% FBS was added to the cells. After incubation for another 4 days, the culture medium was harvested and the cells were examined for the presence of rescued virus under a fluorescence microscope (AMG, USA) using FITC-conjugated antibodies against the RABV N protein.

Virus propagation and titration

All RABV strains were propagated in BSR cells. For virus titration by direct fluorescent antibody assay (dFA), BSR cells in 96-well plates were infected with serial 10-fold dilutions of the virus in DMEM and incubated at 37 °C for 2 days and then moved to 34 °C for another 2 days.

Multi-step growth assays

Monolayer cultures of 2×10^6 BSR cells or NA cells in 9-cm cell culture dish were infected with virus at a multiplicity of infection (MOI) of 0.01 fluorescent focus units (FFU). Virus was adsorbed in 4 ml of growth medium for 1 h and then the cells were washed thrice with PBS. Fresh growth medium was then added into the cells and incubated at 37 °C. Samples of culture medium were harvested at days 1, 2, 3, 4, and 5 post-inoculation. Virus titer was determined in BSR cells by the dFA as previously described.

Interferon expression analysis using ELISA

BSR cells were infected with either the HEP-Flury, or rHEP-CaIFNα1 virus at an MOI of 0.1, 0.5, or 1.0, respectively. After incubation at 37 °C for 24 h, the culture supernatants were harvested. Concentrations of CaIFNα1 in cell-free cell culture supernatants were determined using an ELISA kit for canine interferon alpha (Cloud-Clone, USA), according to the manufacturer's instructions.

CaIFNα1 treatment assay and immunofluorescence microscopy

To confirm the sensibility of mouse to canine interferon α1 (CaIFNα1), BSR cells, NA cells, and Balb/c-3T3 cells were seeded in a glass bottom cell culture dish (NEST, China) and were incubated with 500 U/ml CaIFNα1 (Pichia pastoris source, prepared by our laboratory) at 37 °C for 1 h. Mock treatment was conducted by inoculation with DMEM. After incubation step, the cells were fixed using Immunol Staining Fix Solution (Beyotime, China) for 10 min at room temperature and were permeabilized in 0.5% TritonX-100 (Amresco, USA) in phosphate-buffered saline (PBS). After incubation with pSTAT1(Y701)-PE (1:20 in PBS for 1 h at 37 °C), nuclecular chromatin was stained by adding 4′,6-diamidino-2-phenylindole (DAPI) (Beyotime, China).

Confocal laser scanning microscopy was performed with a Zeiss LSM780 laser system using a Zeiss LSCM 7DUO microscope. Excitation of Alexa Flour 488 nm, PE and DAPI occurred at wavelengths of 575 nm, and 460 nm, respectively. To avoid cross talk, the individual channels were scanned sequentially.

Apoptosis assay

To investigate the influence of canine interferon expressing by rRABV on infected cells in vitro, detection of apoptosis by cytometry analysis of annexin-V and propidium iodide (PI) staining was conducted using Annexin V-FITC Apoptosis Detection Kit (Keygentec, China). BSR cells and NA cells were infected with either the HEP-Flury, or rHEP-CaIFNα1 at an MOI of 1.0, respectively. After infected with virus for 24 h, both floating and adherent cells were collected and processed as recommended by the manufacturer. Flow cytometry was performed using a Beckman FC 500 flow cytometer (Beckman Coulter, USA). Data were analyzed using FCS Express 4 flow cytometry (De Novo Software, USA).

Animal experiments

Chinese Kun Ming (KM) mice and BALB/c mice were used in this research. For the pathogenicity study, BALB/c mice (6–7 weeks of age) were infected intracranially with 10^5 FFU of either the HEP-Flury, rHEP-CaIFNα1 or with medium alone (mock infection). Body weight was monitored daily. Data were obtained from 5 mice in each group for 30 days and presented as the mean value ± standard error (SE). To investigate the immunogenicity of recombinant RABV expressing CaIFNα1, groups of 10 KM mice (6–7 weeks of age) were immunized via the intramuscular route with serial 10-fold dilutions of HEP-Flury, or rHEP-CaIFNα1. At days 7, 14, and 21 after immunization, peripheral blood was obtained, and the serum was used to determine virus neutralizing antibody (VNA) titers, using an ELISA assay (Synbiotics, USA), according to the manufacturer's instructions. At day 23 after immunization, mice were challenged intracranially with 50 LD_{50} CVS-24 and observed daily for 2 weeks. The number of survivors was recorded and compared. Data were analyzed using GraphPad Prism 5 (GraphPad software, USA) with Gehan–Breslow–Wilcoxon Test or Log-rank (Mantel–Cox) Test.

Quantitative real-time PCR

To evaluate interferon-induced gene expression at the inoculation site, BALB/c mice (6–7 weeks of age) were inoculated via the intramuscular route in the right hind leg with 10^5 FFU of one of the recombinant viruses or with medium alone. After the mice were humanely sacrificed, the right hind leg muscles of 4 mice from each group were removed from infected mice at days 3 and 6 post-infection and flash frozen in liquid nitrogen before being stored at −80 °C. Total RNA was extracted using SV Total RNA Isolation (Promega, USA) and used for first strand cDNA synthesis (Roche, GER) following the manufacturer's protocols. Each reaction was carried out in triplicate using SsoAdvanced SYBR Green Supermix (Bio-Rad, USA) according to the manufacturer's instructions. The real-time SYBR Green PCR assay was carried out in a CFX384 Real-Time System (Bio-Rad, USA). The expression levels of target genes, IIGP1, IRF3, PDCD4, STAT1, and mouse interferon alpha (MusIFNα1), were normalized to those of the reference gene glyceraldehyde-3-phosphate dehydrogenase (GAPDH). In order to analyze whether interferon-induced responses affected viral growth in vivo, the RABV N mRNA and CaIFNα1 mRNA were

Table 1
Primers used for amplifying target and reference genes.

Gene	Right primer (5′–3′)	Left primer (5′–3′)
MusIFN	TCAGTCTTCCCAGCACATTG	GAGAAGAAACACAGCCCCTG
IIGP1	GCAATGCCATTCTCCCTAAA	AATGAAGCAGATGGCAAACC
IRF3	ACCGGAAATTCCTCTTCCAG	GATGGCTGACTTTGGCATCT
ISG20	GGCATCTTCCACAGAGCAGT	TACTACAGCCGAGTGTCCCTG
PDCD4	AAGGCTAAGGACACTGCCAA	CAGGAATACTTTGAGCATGGAG
STAT1	CTGAATATTTCCCTCCTGGG	TCCCGTACAGATGTCCATGAT
GADPH	TTGATGGCAACAATCTCCAC	CGTCCCGTAGACAAAATGGT
RABV N	GAGTTGTCATCAGGGTGTGGT	ACATTGCGGATAGAATAGAGCAG
CaIFNα1	CGATCTCGGCTCTCACCATC	AGCACCCTGAGGACCTACTT

quantitated relative to the GAPDH expression level. The primers used to amplify target and reference genes are listed in Table 1. Levels of interferon-induced gene expression in a test sample are presented as the fold increase over those detected in sham-infected controls.

Flow cytometry

To investigate effects of CaIFNα1 expression on the recruitment of T cells in the peripheral blood and B cells in lymph nodes, flow cytometry was performed using a Beckman FC 500 flow cytometer (Beckman Coulter, USA). Briefly, female BALB/c mice of 6–7 weeks of age were inoculated intramuscularly with 10^5 FFU of one of the recombinant RABVs or with medium alone. At days 3, 5, and 7 post-infection, the single-cell suspension of peripheral blood or inguinal lymph nodes was harvested and stained with antibodies to T cell- (FITC-CD3e, PerCP-CD4, and PE-CD8a) or B cell- (FITC-CD19 and PE-CD40)markers (BD Biosciences Pharmingen, USA) for 15 min at room temperature (20–25 °C). A minimum of 100,000 events were counted. Data were analyzed using FCS Express 4 flow cytometry (De Novo Software, USA).

Statistical analysis

All experiments were repeated at least three times. Data were analyzed using GraphPad Prism 5 (GraphPad software, USA), or one-way ANOVA. $P < 0.05$ was considered a significant difference. For all tests, the following notations are used to indicate significance between groups: $*p < 0.05$; $**p < 0.01$; $***p < 0.001$.

Funding statement

This study was partially supported by Special Fund for Agro-Scientific Research in the Public Interest (No. 201103032) and Research of Guangdong Province and Ministry of Education (No. 2010A090200083).

References

Ahlenstiel, G., Edlich, B., Hogdal, L.J., Rotman, Y., Noureddin, M., Feld, J.J., Holz, L.E., Titerence, R.H., Liang, T.J., Rehermann, B., 2011. Early changes in natural killer cell function indicate virologic response to interferon therapy for hepatitis C. Gastroenterology 141, 1231–1239.
Baloul, L., Lafon, M., 2003. Apoptosis and rabies virus neuroinvasion. Biochimie 85, 777–788.
Braun, D., Caramalho, I., Demengeot, J., 2002. IFN-α/β enhances BCR-dependent B cell responses. Int. Immunol. 14, 411–419.
Carty, M., Reinert, L., Paludan, S.R., Bowie, A.G., 2014. Innate antiviral signalling in the central nervous system. Trends Immunol. 35, 79–87.
Castigli, E., Young, F., Carossino, A.M., Alt, F.W., Geha, R.S., 1996. CD40 expression and function in murine B cell ontogeny. Int. Immunol. 8, 405–411.
Chopy, D., Detje, C.N., Lafage, M., Kalinke, U., Lafon, M., 2011. The type I interferon response bridles rabies virus infection and reduces pathogenicity. J. Neurovirol. 17, 353–367.
Cox, M.A., Kahan, S.M., Zajac, A.J., 2013. Anti-viral CD8 T cells and the cytokines that they love. Virology 435, 157–169.
Degols, G., Eldin, P., Mechti, N., 2007. ISG20, an actor of the innate immune response. Biochimie 89, 831–835.
Faul, E.J., Lyles, D.S., Schnell, M.J., 2009. Interferon response and viral evasion by members of the family Rhabdoviridae. Viruses 1, 832–851.
Faul, E.J., Wanjalla, C.N., McGettigan, J.P., Schnell, M.J., 2008. Interferon-β expressed by a rabies virus-based HIV-1 vaccine vector serves as a molecular adjuvant and decreases pathogenicity. Virology 382, 226–238.
Fink, K., Lang, K.S., Manjarrez-Orduno, N., Junt, T., Senn, B.M., Holdener, M., Akira, S., Zinkernagel, R.M., Hengartner, H., 2006. Early type I interferon-mediated signals on B cells specifically enhance antiviral humoral responses. Eur.J. Immunol. 36, 2094–2105.
Gomme, E.A., Wanjalla, C.N., Wirblich, C., Schnell, M.J., 2011. Rabies virus as a research tool and viral vaccine vector. Adv. Virus Res. 79, 139.
Hicks, D., Fooks, A., Johnson, N., 2012. Developments in rabies vaccines. Clin. Exp. Immunol. 169, 199–204.
Inoue, K.-i., Shoji, Y., Kurane, I., Iijima, T., Sakai, T., Morimoto, K., 2003. An improved method for recovering rabies virus from cloned cDNA. J. Virolog. Methods 107, 229–236.
Ivashkiv, L.B., Donlin, L.T., 2014. Regulation of type I interferon responses. Nat. Rev. Immunol. 14, 36–49.
Kalliolias, G.D., Ivashkiv, L.B., 2010. Overview of the biology of type I interferons. Arthritis Res. Ther. 12, S1.
Kohlmeier, J.E., Cookenham, T., Roberts, A.D., Miller, S.C., Woodland, D.L., 2010. Type I interferons regulate cytolytic activity of memory $CD8^+$ T cells in the lung airways during respiratory virus challenge. Immunity 33, 96–105.
Kotredes, K.P., Gamero, A.M., 2013. Interferons as inducers of apoptosis in malignant cells. J. Interferon Cytokine Res. 33, 162–170.
Kuang, Y., Lackay, S.N., Zhao, L., Fu, Z.F., 2009. Role of chemokines in the enhancement of BBB permeability and inflammatory infiltration after rabies virus infection. Virus Res. 144, 18–26.
Lafon, M., 2011. Evasive strategies in rabies virus infection. Adv. Virus Res. 79, 33.
Le Bon, A., Thompson, C., Kamphuis, E., Durand, V., Rossmann, C., Kalinke, U., Tough, D.F., 2006. Cutting edge: enhancement of antibody responses through direct stimulation of B and T cells by type I IFN. J. Immunol. 176, 2074–2078.
Leroy, M., Pire, G., Baise, E., Desmecht, D., 2006. Expression of the interferon-alpha/beta-inducible bovine Mx1 dynamin interferes with replication of rabies virus. Neurobiol. Dis. 21, 515–521.
Lieu, K.G., Brice, A., Wiltzer, L., Hirst, B., Jans, D.A., Blondel, D., Moseley, G.W., 2013. The rabies virus interferon antagonist P-protein interacts with activated STAT3 and inhibits Gp130 receptor signaling. J. Virol. 87, 8261–8265.
Liu, X.H., Yang, Y., Sun, Z.J., Chen, J., Ai, J., Dun, C., Fu, Z.F., Niu, X.F., Guo, X.F., 2014. A recombinant rabies virus encoding two copies of the glycoprotein gene confers protection in dogs against a virulent challenge. Plos ONE 9, e87305.
Marschalek, A., Finke, S., Schwemmle, M., Mayer, D., Heimrich, B., Stitz, L., Conzelmann, K.-K., 2009. Attenuation of rabies virus replication and virulence by picornavirus internal ribosome entry site elements. J. Virol. 83, 1911–1919.
Niu, X., Tang, L., Tseggai, T., Guo, Y., Fu, Z.F., 2013. Wild-type rabies virus phosphoprotein is associated with viral sensitivity to type I interferon treatment. Arch. Virol., 1–9.
Niu, X., Wang, H., Fu, Z.F., 2011. Role of chemokines in rabies pathogenesis and protection. Adv. Virus Res. 79, 73.
World Health Organization, 2010. WHO Expert Consultation on Rabies: First Report. World Health Organ. Tech. Rep. Ser., World Health Organization.
Randall, R.E., Goodbourn, S., 2008. Interferons and viruses: an interplay between induction, signalling, antiviral responses and virus countermeasures. J. Gen. Virol. 89, 1–47.
Rieder, M., Conzelmann, K.-K., 2011. Interferon in rabies virus infection. Adv. Imaging Electron Phys. 79, 91–114.
Schnell, M.J., McGettigan, J.P., Wirblich, C., Papaneri, A., 2009. The cell biology of rabies virus: using stealth to reach the brain. Nat. Rev. Microbiol. 8, 51–61.
Schoggins, J.W., Wilson, S.J., Panis, M., Murphy, M.Y., Jones, C.T., Bieniasz, P., Rice, C. M., 2011. A diverse range of gene products are effectors of the type I interferon antiviral response. Nature 472, 481–485.
Schutsky, K., Curtis, D., Bongiorno, E.K., Barkhouse, D.A., Kean, R.B., Dietzschold, B., Hooper, D.C., Faber, M., 2013. Intramuscular inoculation of mice with the live-attenuated recombinant rabies virus TriGAS results in a transient infection of the draining lymph nodes and a robust, long-lasting protective immune response against rabies. J. Virol. 87, 1834–1841.
Sen, A., Pruijssers, A.J., Dermody, T.S., García-Sastre, A., Greenberg, H.B., 2011. The early interferon response to rotavirus is regulated by PKR and depends on MAVS/IPS-1, RIG-I, MDA-5, and IRF3. J. Virol. 85, 3717–3732.
Staudt, V., Bothur, E., Klein, M., Lingnau, K., Reuter, S., Grebe, N., Gerlitzki, B., Hoffmann, M., Ulges, A., Taube, C., 2010. Interferon-regulatory factor 4 is essential for the developmental program of T helper 9 cells. Immunity 33, 192–202.
Subedi, A., Kim, M.J., Nepal, S., Lee, E.-S., Kim, J., Sohn, D.-H., Song, K., Lee, S.H., Park, W.S., Jeong, B.-S., 2013. Globular adiponectin modulates expression of programmed cell death 4 and miR-21 in RAW 264.7 macrophages through the MAPK/NF-κB pathway. FEBS Lett..
Taira, O., Watanugi, I., Hagiwara, Y., Takahashi, M., Arai, S., Sato, H., Maehara, N., 2005. Cloning and expression of canine interferon-alpha genes in Escherichia coli. J. Vet. Med. Sci.: Jpn. Soc. Vet. Sci. 67, 1059.

Uthaiah, R.C., Praefcke, G.J., Howard, J.C., Herrmann, C., 2003. IIGP1, an interferon-γ-inducible 47-kDa GTPase of the mouse, showing cooperative enzymatic activity and GTP-dependent multimerization. J. Biol. Chem. 278, 29336–29343.
Verardi, P.H., Titong, A., Hagen, C.J., 2012. A vaccinia virus renaissance: new vaccine and immunotherapeutic uses after smallpox eradication. Hum. Vaccines Immunother. 8, 961–970.
Vidy, A., El Bougrini, J., Chelbi-Alix, M.K., Blondel, D., 2007. The nucleocytoplasmic rabies virus P protein counteracts interferon signaling by inhibiting both nuclear accumulation and DNA binding of STAT1. J. Virol. 81, 4255–4263.
Wang, H., Zhang, G., Wen, Y., Yang, S., Xia, X., Fu, Z.F., 2011. Intracerebral administration of recombinant rabies virus expressing GM-CSF prevents the development of rabies after infection with street virus. Plos ONE 6, e25414.
Wen, Y., Wang, H., Wu, H., Yang, F., Tripp, R.A., Hogan, R.J., Fu, Z.F., 2011. Rabies virus expressing dendritic cell-activating molecules enhances the innate and adaptive immune response to vaccination. J. Virol. 85, 1634–1644.
Wiltzer, L., Okada, K., Yamaoka, S., Larrous, F., Kuusisto, H., Sugiyama, M., Blondel, D., Bourhy, H., Jans, D., Ito, N., 2014. Interaction of rabies virus P-protein with STAT proteins is critical to lethal rabies disease. J. Infect. Dis. 209, 1744–1753.
Yilma, T., Verardi, P., Jones, L., 2010. Development of safe and effcacious viral vaccines for animals. Crit. Rev. Immunol., 30.
Zhang, G., Wang, H., Mahmood, F., Fu, Z.F., 2012. Rabies virus glycoprotein is an important determinant for the induction of innate immune responses and the pathogenic mechanisms. Vet. Microbiol..
Zhang, G., Zhang, Z., Liu, Z., 2013. Interferon regulation factor-3 is a critical regulator of the mature of dendritic cells from mice. Scand. J. Immunol. 77, 13–20.
Zhang, N., Bevan, M.J., 2011. $CD8^+$ T cells: foot soldiers of the immune system. Immunity 35, 161–168.
Zhao, L., Toriumi, H., Wang, H., Kuang, Y., Guo, X., Morimoto, K., Fu, Z.F., 2010. Expression of MIP-1α (CCL3) by a recombinant rabies virus enhances its immunogenicity by inducing innate immunity and recruiting dendritic cells and B cells. J. Virol. 84, 9642–9648.